DTU Library

How To Design for a Tailored Subcellular Distribution of Systemic Agrochemicals in Plant Tissues

Hofstetter, Sandro; Beck, Andreas; Trapp, Stefan; Buchholz, Anke

[Link back to DTU Orbit](#)

How to design for a tailored subcellular distribution of systemic agrochemicals in plant tissues

Sandro Hofstetter (1), Andreas Beck (1), Stefan Trapp (2), Anke Buchholz (1,*)

[1] Syngenta Crop Protection AG, Schaffhauserstrasse 101, 4332 Stein, Switzerland

[2] Technical University of Denmark, Miljoevej 113, 2800 Kongens Lyngby, Denmark

* anke.buchholz@syngenta.com, Tel +41 62 866 0145, Fax +41 62 866 0864

Running title: Predicting intracellular localization of agrochemicals in plant tissues

1   **Abstract**

2   Foliar applied systemic agrochemicals require the entrance into the plant vascular system or

3   into specific subcellular compartments to reach their target in planta or to be imbibed by

4   piercing-sucking pests. An inappropriate subcellular localization, like accumulation of

5   aphicides in vacuoles, might lower compound efficiency due to reduced exposure to the

6   target.

7   Permeabilities and mass distributions of sixteen compounds covering a broad range of

8   properties were measured across a pH gradient in a PAMPA ('Parallel artificial membrane

9   permeability assay') system, providing experimental evidence for ion trapping of acids and

10   bases in basic and acidic compartments, respectively. The results validated a predictive

11   model which was then expanded to simulate a standardized plant cell (cytosol and vacuole)

12   with vascular system (phloem and xylem).

13   This approach underlined that the absolute mass distribution across aqueous phases was

14   defined by membrane retention (M_r) whereas the relative mass distribution was determined

15   by the species (neutral, acidic, basic) of compounds. These processes depend largely on pK_a

16   and log K_{ow} of the test compounds, which subsequently determine the partitioning of the

17   substances in plant cell compartments. The validated model can be used as a tool in

18   agrochemistry research to tailor the subcellular distribution by chemistry design and to

19   interpret biology results.

20

21

22   Keywords:

23   PAMPA, intracellular localization model, pH partition hypothesis, vacuole trapping

Introduction

25   Eukaryotic cells have highly organized subcellular compartments with distinct structural and

26   functional features. Plant vacuoles are versatile organelles with a crucial role in

27   osmoregulation, undertaking functions such as recycling, detoxification and storage [14].

28   Different transport processes occur at the vacuolar membrane for inorganic or biotic solutes

29   [30]. The electrochemical and pH gradient generated by channels and transporters might also

30   lead to an accumulation of xenobiotics within this largest cell compartment of mature plant

31   cells.

32   The present study aims to provide experimental evidence for the postulated vacuole

33   trapping of basic pesticides in leaf cells [10, 11, 34].

34   The accumulation of weakly basic compounds in acidic organelles has been observed in

35   animal and human cells [12, 17, 46, 51] and was also recently discovered for acidic vesicles of

36   protozoa [20]. Ion trapping of weakly acidic herbicides leads to phloem transport and systemic

37   translocation in plants [27, 48] and is well described for phytohormones such as auxins [21, 35] and

38   abscisic acid [23]. It is expected that a similar passive mechanism occurs in plant cells, whereby

39   weakly basic compounds are distributed into the large acidic vacuoles. The passive

40   accumulation of alkaloids in acidic latex vacuoles against a concentration gradient was

41   described by Hauser and Wink (1990) [24]. On the macroscale, an increased accumulation of

42   weak bases in plants was observed with increasing pH [25, 36]. But as of yet, no systematic

43   study on the ion trap effect due to pH gradients of weakly alkaline pesticides has been

44   published.

45   Calculations based on first principles indicated that intrinsically very active pesticides might

46   not show sufficient translaminar pest control which is required for a robust field

47   performance against sucking pests after foliar spray if trapping in vacuoles inhibits dose

48 effective translaminar distribution [8]. Especially phloem feeders such as aphids and whiteflies

49 avoid piercing their stylet into the vacuole which contains natural plant defense compounds

50 like alkaloids [22]. Lipophilic compounds may be limited in translaminar diffusive transport, as

51 they stick to membranes and other lipophilic structures [8]. On the other hand, partitioning

52 into membranes favors membrane permeation and thus symplastic transport inside

53 mesophyll cells. Compounds accumulating inside of cells could be imbibed by cell feeders

54 like thrips and mites. The design for specific intracellular distribution profiles may thus be

55 seen as a new approach for target selectivity of pesticides [7].

56 Initially we will provide experimental evidence for ion trapping of acids and bases in basic

57 and acidic compartments, respectively. This was done by determining the permeabilities and

58 mass distributions of diverse agrochemicals across a pH gradient between two differentially

59 adjusted compartments in a 'Parallel artificial membrane permeability assay' (PAMPA). The

60 permeabilities were measured in a kinetic and equilibrium approach.

61 In a second step we will compare the measured mass fractions with the postulated

62 distributions as calculated with a cell model [50, 51]. This model is gradually expanded to a four

63 compartment model representing a standardized plant cell (cytosol and vacuole) and plant

64 vascular system (phloem and xylem).

65 This paper provides results on a broad range of chemistry and also validates a model that

66 allows to interpret and to predict intracellular localization. This knowledge on subcellular

67 localization of new active ingredients in plant cells can be exploited for selective targeting of

68 pests and is an essential element in research of modern agrochemistry.

69

70 **Material and Methods**

4

71 **Reagents.** Sixteen compounds comprising monoprotic weak acids, monoprotic weak bases

72 and neutral compounds and differing in acid dissociation (pK_a) and lipophilicity were selected

73 for the experiments. This set of compounds included diverse chemistries including

74 commercial agrochemicals, research compounds and the reference drug carbamazepine.

75 The commercial insecticides pymetrozine (PYME), thiamethoxam (THMX), cyantraniliprole

76 (CYNT), spirotetramat (SPAT) and its free acid, spirotetramat enol (SPAT enol) as well as the

77 research compounds oxazoline (OX), imidazoline (IM) and additional research compounds

78 (compd 1 to compd 8), which were synthesized in house. Carbamazepine (CBZ), DMSO

79 (analytical grade), formic acid, acetonitrile (HPLC grade), methanol (HPLC grade) were

80 obtained from Sigma-Aldrich (St Louis, MO).

81 The chemical structures of the compounds are shown in Figure 1. The name, abbreviation,

82 molecular weight, pK_a, log K_{ow} as well as log D (calculated) of test compounds are shown in

83 Table 1. Physicochemical properties were either taken from literature or

84 measured/calculated in-house. All weak bases had a pK_a well above 7.0 whereas the weak

85 acids possessed a pK_a well below 5.5. The log K_{ow} ranged from -0.2 to 6.8.

86 The water used in this study was purified (> 18 MΩ cm) with Milli-Q Advantage A10 from

87 Millipore (Merck KGaA, Darmstadt, Germany).

88

89 **Parallel artificial membrane permeability assay (PAMPA).** PAMPA evaluation software

90 (PAMPA Explorer version 3.7.2) and Gutbox^{TM} were used from Pion (Billerica, MA). Donor

91 plates (Multiscreen Transport Receiver Plate, MATRNPS50), acceptor plates (Multiscreen-IP,

92 MAIPN4550, pore size 0.45 µm) and filtration plates (Multiscreen-HV, MSHVN4550, 0.45 µm

93 pore size) were purchased from Millipore (Merck KGaA, Darmstadt, Germany). Flat bottom

94 UV-plates (reference plate) were obtained from Thermo-Fisher (Waltham, MA). Dodecane

95   (reagentPlus), MES and HEPES buffer were acquired from Sigma Aldrich (St Louis, MO). L-α-

96   phosphatidylcholine from egg yolk (ca. 60%; TLC grade) from Sigma Aldrich (St Louis, MO)

97   was not further purified and stored at -20 °C prior to use. The phospholipid solution was

98   prepared before usage as 10% (w/v) phosphatidylcholine in dodecane. All test compounds

99   were prepared as 10'000 mg/L stock solution in DMSO. The test solutions were further

100 diluted with 50 mM MES (pH 5.5) or HEPES buffer (pH 7.0) to 50 mg/L, keeping the final

101 DMSO concentration below 1% (v/v) and filtered through a filtration plate (0.45 µm pores)

102 prior to usage to ensure a homogenous solution.

103 PAMPA was performed in 96 well plates as described elsewhere [16, 32]. The PAMPA sandwich

104 assembly contained a donor plate and an acceptor plate creating two chambers separated

105 by a microfilter disc (Figure 2). The filter disc was coated with 5 µL of phospholipid solution

106 and dried for 30 min. The Tecan freedom EVO liquid handler transferred an aliquot from the

107 test solutions into the donor plate and reference plate. The acceptor plate was prepared

108 with acceptor buffer and the PAMPA sandwich was assembled together with the donor

109 plate. Incubation occurred at room temperature under constant humidity in the Gut-Box[TM].

110 The PAMPA sandwich was disassembled after incubation and an aliquot of both acceptor

111 and donor solution was quantified. The compound distribution between donor, acceptor and

112 the remaining fraction in the filter was compared to a reference sample which was directly

113 measured after initiation of incubation.

114 Compounds in the permeability assay were measured under a bidirectional pH sink

115 condition, initially having pH 7.0 in the acceptor plate and pH 5.5 in the donor plate, and

116 following these measurements the pH gradients was reversed. These pH values were chosen

117 to mimic an ideal plant cell simplified to two equally sized compartments, the cytosol

118 (pH 7.0) and the embedded vacuole (pH 5.5). This gradient is more pronounced than

119 common applications in pharma where the blood (pH 7.4) and small intestine (pH 6.5) are

120 mimicked [26]. A test series generally contained DMSO as a blank and carbamazepine as an

121 internal reference standard. Compounds were measured in triplicates in each run.

122

123 **Kinetic approach.** The permeability of the compounds was tested across a pH gradient from

124 pH 7.0 to pH 5.5 and *vice versa*. The assay was done without any additional sink condition in

125 the acceptor compartment (e.g. sodium dodecyl sulfate [1]) and performed without stirring [3].

126 The majority of investigated compounds displayed moderate hydrophobicity, i.e. log D (pH

127 5.5 / 7.0) ≤ 2.5, supposing unaffected permeability through the membrane (except compd 1,

128 2, 7 and 8). Inside living cells the cytosol streaming would largely eliminate unstirred

129 boundary layers, whereas in the PAMPA system unstirred boundary layers may provide

130 additional resistance. However, the effect of the unstirred boundary layer is minor

131 compared to the resistance of the artificial membrane layer with a thickness of 125 µm [2],

132 except for the highly lipophilic compounds [9].

133 In the kinetic approach, the incubation time was 18 h and quantification was performed by

134 UV spectrum (230 - 500 nm) analysis. The effective permeability (P_e) was measured by

135 UV/Vis spectra (TECAN® infinite M200pro) and evaluated with the PAMPA evaluation

136 software (PAMPA Explorer, Pion) [29].

137

138 **Equilibrium approach.** In this thermodynamic approach (phase equilibrium condition), the

139 PAMPA sandwich was incubated for six days without stirring. After this incubation period,

140 the mass fractions in the donor and acceptor compartment were measured by UPLC (ultra-

141 performance liquid chromatography) mass spectrometer. All other conditions were identical

142 to the kinetic approach. During this time it is expected that equilibrium is established due to

143 the small size of the system (600 µL). Equilibrium for neutral compounds means identical

144 concentrations in the donor and acceptor compartment, whereas higher concentrations are

145 expected in the alkaline and the acidic compartment for weak acids and weak bases,

146 respectively.

147 Compound concentrations were determined by UPLC-MS/UV. The UV/MS (ultraviolet / mass

148 spectrum) signal was recorded with Agilent 1200 UPLC system (Agilent Technologies, Santa

149 Clara, CA) equipped with an Acquity UPLC BEH C18 (2.1 x 50 mm, 1.7 µm) column at 60 °C

150 (Table S1). The mobile phase consisted of (A) HPLC grade water with 0.5% methanol and

151 0.05% formic acid and (B) acetonitrile with 0.05% formic acid. The elution started with a

152 mobile phase of 95% A for 12 s followed by a linear gradient to 100% B over 72 s. The mobile

153 phase was then changed gradually to 70% B for 40 s and returned to 5% B in the end. Peak

154 finding and peak area quantification was performed by using XCalibur 3.0 software (Thermo

155 Fischer Scientific).

156

157 **Mass distributions across donor and acceptor compartment.** Compartments could be either

158 considered as a real biological cell compartments (an aqueous phase surrounded by a

159 membrane) or as the bioavailability determining compartment (restriction to the aqueous

160 phase). The latter is the case if the aqueous phase reflects the dose limiting factor to control

161 e.g. sucking pests.

162 If donor and acceptor are considered as a biological cell compartment, the membrane

163 retention (M_r) is included in each phase. Masses in donor (M_d) and acceptor (M_a) were

164 quantified and the membrane retention (M_r) was derived by the mass balance; whereas

165 (M_{ref}) was the total mass in the reference plate:

166

167 $$M_r = M_{ref} - M_d - M_a \qquad\qquad\qquad (1)$$

168

169 The mass fraction of donor (%M_d) was calculated as follows (Table S2):

170

171 $$\%M_d = 100 \times \frac{M_d}{(M_d + M_a + M_r)} \qquad\qquad (2)$$

172

173 Mass fractions for acceptor (%M_a) and membrane retention (%M_r) were calculated

174 accordingly.

175 If donor and acceptor compartments were restricted to their aqueous phase, the mass

176 fraction of e.g. donor (%$M_{d,aq}$) was calculated neglecting the membrane retention:

177

178 $$\%M_{d,aq} = 100 \times \frac{M_d}{M_d + M_a} \qquad\qquad (3)$$

179

180 **Permeability with ion trapping conditions and related calculation of mass fractions.** Weak

181 acids and bases have two relevant molecule species that diffuse in the system, namely the

182 neutral and the ionic species. The movement of ionized molecules across charged

183 membranes is described by the Nernst-Planck equation [48], when the electrical potential

184 approaches zero, the equation converges to Fick's Law of diffusion. In living cells, the ATPase

185 creates a resting potential of about -100 mV at the outer membrane. Artificial systems with

186 phosphatidylcholine membranes (PAMPA) have no ATPase. A small net charge can

187 theoretically be generated due to the diffusion of buffers and electrolytic test compounds

188 across the membrane (Goldman-Hodgkin-Katz-equation[19, 45]) but we do not expect this to

189   have a significant effect. We therefore neglect electrical charge at the membranes and

190   calculate with Fick's 1st Law of diffusion. Accordingly, the overall exchange across the

191   membrane is the net exchange of both molecule species:

192

193
$$\frac{dm}{dt} = A\,P_n(a_{n,d} - a_{n,a}) + A\,P_i(a_{i,d} - a_{i,a}) = A\,P_{e,da}C_d - A\,P_{e,ad}C_a \tag{4}$$

194

195   dm/dt is the exchange of chemical mass from donor to acceptor, A is the exchange area

196   (membrane cross-area, cm^2), P (cm/s) is permeability (of n neutral species and i ion) and a is

197   chemical activity in the donor (d) and acceptor (a) compartment. P_e is the effective

198   permeability, composed of the permeability of the neutral and of the ionic species, from

199   donor to acceptor (subscript da) or from acceptor to donor (subscript ad) compartment. For

200   dilute aqueous solutions, activity a is approximately the same as concentration C in solution.

201   The effective permeability P_e depends on the individual permeabilities of the neutral or the

202   ionic species at a given pH. In case of steady-state, the ratio between concentrations of both

203   compartments corresponds to the ratio of effective permeabilities. For equal volumes of

204   donor and acceptor compartment, the concentration ratio is identical to the mass ratio, and

205   Equation 5 follows Krämer (2016) [28]:

206

207
$$\frac{M_{a,Eq}}{M_{d,Eq}} = \frac{P_{e,da}}{P_{e,ad}} \tag{5}$$

208

209   The charged species has a membrane permeability which is orders of magnitude slower than

210   the neutral species [49]. Therefore, the solute is trapped in the compartment where the

211   molecule is ionized, i.e., acids at higher pH and bases at lower pH [51]. In general, ion trapping

212   only reduces P_e in the direction from the compartment with trapping to the one without [28].

213   In the absence of other diffusive processes, this mass ratio in steady-state equals the

214   thermodynamic phase equilibrium, i.e. the endpoint of diffusion which is the system state

215   with the highest entropy. Therefore, we determined P_e under both trapping conditions as

216   forward permeability ($P_{e,fw}$) from pH 7.0 to pH 5.5 and as reverse permeability ($P_{e,rv}$) at

217   steady state (i.e. determined after 18 h) (Equation 6 and 7):

218

$$donor\ (pH\ 7.0) \xrightarrow{P_e(fw)} acceptor(pH\ 5.5) \tag{6}$$

220

$$donor\ (pH\ 5.5) \xrightarrow{P_e(rv)} acceptor(pH\ 7.0) \tag{7}$$

222

223   The real mass fractions in donor and acceptor compartment (i.e. in aqueous phases) at

224   equilibrium (%$M_{a,eq}$ and %$M_{d,eq}$) are obtained by considering the membrane retention (%M_r)

225   and reflecting the different directions of permeabilities ($P_{e,fw}$ and $P_{e,rv}$); as shown in Equation

226   8 and 9.

$$\%M_{a,eq} = (100 - \%M_r) \times \frac{P_{e,fw}}{P_{e,fw} + P_{e,rv}} \tag{8}$$

$$\%M_{d,eq} = (100 - \%M_r) \times \frac{P_{e,rv}}{P_{e,fw} + P_{e,rv}} \tag{9}$$

229   Accordingly, our calculations for the relative mass distribution in donor and acceptor at

230   equilibrium were done with the membrane retention as measured in the equilibrium

231 approach and with the forward and reverse permeability as measured in the kinetic

232 approach.

233

234 **Cell model and adaptations.** The cell model has been used for a number of applications in

235 medicine [46, 50, 51], and it was also coupled to transport models of pesticides in plants [8, 47].

236 Here, we test and apply its core element, the model for intracellular distribution [48]. The

237 chemical input parameters, log K_{ow} neutral, log K_{ow} ion, pK_a, MW and the valency (charge

238 number) are shown in Table 1. The valency is +1 for bases (OX, IM and compd 3 to compd 8)

239 and -1 for acids (SPAT enol, compd 1 and compd 2).

240 The cell model parameters were adapted to reflect the conditions in our PAMPA test system

241 (Table S3): Only two compartments were considered (donor and acceptor). The volume of

242 the donor (= cytosol) and the acceptor (= vacuole) were equally sized with a total volume of

243 600 μL. The applied L-α-phosphatidylcholine concentration defined the lipid to water ratio as

244 0.83% to 99.17%. The membrane potential was set to 0.01 V. Equilibration started from the

245 cytosol (donor) and the mass distribution in the cytosol and vacuole were calculated for

246 $t = \infty$ after incubation start. The membrane retention represented the sum of both lipid

247 fractions of both compartments, plasmalemma (cytosol) and tonoplast (vacuole).

248

249 **Extension of the cell model to the four compartment model for plant tissues.** A predictive

250 model for localization of pesticides in cell compartments and transfer in plant tissues has

251 been described recently [8]. Thus far, the measured or predicted mass fractions in the 'PAMPA

252 cell model' cannot be directly translated to an *in planta* environment. For a direct

253 comparison the relative dimensions of different compartments and thickness (i.e. thinner) of

254 the biomembrane would have to be considered. These respective parameters are listed in

255 Table S3. This model includes besides both major cell compartments, the cytosol (pH 7.2)

256 and the vacuole (pH 5.5), but also both elements of the plant vascular system, the xylem (pH

257 5.5) and phloem (pH 8.0). This model approach only considered the cytosol and the vacuole

258 as compartments containing a lipid fraction, i.e. being surrounded by the plasmalemma and

259 tonoplast. Compounds in the lipid phase ('at lipids' fraction) or dissolved in the aqueous

260 phase ('solved' fraction) were therefore calculated separately for each cell compartment,

261 whereas the mass fraction in the xylem and phloem were exclusively described as the solved

262 fraction.

263

264 **Results**

265 **Kinetic measurements.** The permeability measurements were done under steady state

266 conditions (i.e. at constant kinetics) and indicated the preferred permeation direction with

267 different pH gradient conditions. Neutral compounds exhibited equal permeabilities (P_e) in

268 both pH gradient directions (Figure 3) within a range of 0.19 ($\pm$ 0.01) $\times$ 10^{-6} to 11.45 ($\pm$ 1.05)

269 $\times$ 10^{-6} cm/s (Table 2). The permeation of acidic compounds from pH 5.5 to pH 7.0 was in

270 average 40 times faster than in the opposite direction. All basic compounds permeated

271 faster from pH 7.0 to pH 5.5 by about factor 40; except for compd 3 which had similar

272 permeability in both pH gradients. Compd 3 is the most hydrophilic compound with a log D

273 of -3.6 at pH 5.5. Surprisingly it demonstrated very low permeability, close to the minimal

274 detection limit in both pH gradient directions. Previous investigations on other basic

275 hydrophilic compounds with bidirectional low permeabilites, proposed that ion-pair

276 mediated transport may explain this observation [42-44]. The permeability of the very lipophilic

277 compd 7 and compd 8 could not be measured.

278

Verification of measurements using the pH-partition hypothesis. Before further data

analysis, we had to exclude that exceptional anomalies of ionized species had affected our

permeability measurements. Experimental deviation could derive e.g. from an unstirred

aqueous boundary layer effect. Smolen (1973) [41] demonstrated that pH and pK_a showed the

same relationship as log D. Therefore we plotted the difference in log D between acidic and

basic compartment (Δ log D) and the difference of log P_e from pH 5.5 to pH 7.0 and *vice

versa* (Δ log P_e). The comparative fit with the ideal line (slope of -1 and the intercept is at

zero) would validate the concept of pH partitioning across the membrane (Figure 4).

SPAT enol, as an example, demonstrated a log P_e of -5.9 (direction pH 5.5 to pH 7.0) and

log P_e of -7.4 (direction pH 7.0 to pH 5.5) resulting in a Δ log P_e of 1.5. The corresponding Δ

log D was 1.5 with a log D of 1.7 (pH 5.5) and 0.4 (pH 7.0) in the donor and acceptor

compartment. Typically, neutral compounds exhibited no difference in log D in buffer

solutions with pH 7.0 or pH 5.5, resulting in no difference in log P_e. In contrary, most acids

and bases were confronted with a Δ log D of about 1.5 which was reflected in a Δ log P_e of

1.5 units.

Despite similar pKa as the other basic compounds, compound 3 behaved different and

showed similar permeabilities in both directions. This is likely due to an ion pairing

mechanism which allows ion pairs to cross membranes uncharged and thus as fast as the

neutral species.

Overall, we can state that the measured permeabilities of most test compounds were in

good alignment with the pH partitioning hypothesis (Smolen 1973), which also means that

the permeability of ions did not significantly contribute to the overall membrane

permeability.

303 **Equilibrium measurements.** The neutral compounds, CYNT and SPAT, exhibited equal

304 distribution (50:50) between donor and acceptor for both pH gradient directions indicating

305 complete equilibration (Figure 5). The polar neutral compounds, PYME and THMX, showed

306 an unequal mass balance after six days favoring the donor compartment, independent of the

307 pH gradient direction. The acidic compounds, compd 1 and compd 2, were almost entirely

308 found in the neutral compartment as reflected by the very low fractions in the acidic

309 compartment. However, for the third acid, SPAT enol, 61% remained in the acidic

310 compartment (Table 2) if the equilibration started from an acidic donor. Most basic

311 compounds (OX, compd 4, compd 6, IM and compd 7) almost exclusively remained in the

312 acidic compartment demonstrating ion trapping irrespective of the direction of the pH

313 gradient. Exceptions were compd 3 (postulated ion pairing, see above), compd 5 and

314 compd 8.

315 Compounds stated as not equilibrated in Table 2 showed an unexpectedly high donor

316 fraction as e.g. for PYME and THMX. Their very low permeabilities of ca. 0.2×10^{-6} cm/s

317 (PYME) and ca. 0.7×10^{-6} cm/s (THMX) indicate a very slow equilibration. Very low

318 permeability was also observed for the acid SPAT enol (($1.30 \pm 0.03) \times 10^{-6}$ cm/s from pH 5.5

319 to pH 7.0) and for the base compd 3 (($0.06 \pm 0.01) \times 10^{-6}$ cm/s from pH 7.0 to pH 5.5). These

320 non-equilibrated compounds had a particularly low log D (Table 1).

321 A considerable amount of compd 5 remained in the neutral donor, when equilibrating from

322 pH 7.0 to pH 5.5, which cannot be explained by a low permeability. The permeability of

323 compd 5, ($8.54 \pm 0.94) \times 10^{-6}$ cm/s, was in the range of other basic compounds as for

324 instance compd 4 with ($9.58 \pm 0.48) \times 10^{-6}$ cm/s and compd 6 with ($9.55 \pm 0.82) \times 10^{-6}$ cm/s.

325 Almost full membrane retention was measured for compd 8 which is obviously related to its

326 high log K_{ow} of about 6.5 (Table 2). The equilibration from pH 7.0 to pH 5.5 was below the

15

327   detection limit for compd 8, suggesting major compound loss during the filtration step

328   because of precipitation.

329   In general, the membrane retention at equilibrium was log K_{ow} dependent showing an

330   increasing membrane fraction with increasing log K_{ow}. Assuming that measured

331   permeabilities and equilibrated mass distributions are directly related to the

332   physicochemical properties of tested compounds, the outcomes should be predictable with

333   the mathematical cell model (see Methods).

334

335   **Adapted cell model predicting compound equilibration in PAMPA test system**. The

336   experimental dimension of our applied PAMPA setup had to be reflected in the cell model. In

337   principal, the model adaptations included the equal volume of donor and acceptor, the

338   applied pH conditions and a modified lipid - water distribution (Table S3). The input

339   parameters, acid dissociation constant, lipophilicity and valency are given for each

340   compound in Table 1.

341   This 'PAMPA cell model' predicted an accumulation of basic compounds in the vacuole,

342   accumulation of acidic compounds in the cytosol and equilibration for neutral compounds

343   (Figure 6 A). Increasing membrane retention was described in correspondence to increasing

344   log K_{ow} of test compounds.

345   The model predictions were compared with the mass distribution at equilibrium (%$M_{a,eq}$ and

346   %$M_{d,eq}$), which could have been taken directly from the equilibrium measurements (Table 2).

347   Since five compounds did not equilibrate within six days, the mass distribution at equilibrium

348   was derived from their measured permeabilities (Equation 8). To be consistent, this

349   extrapolation was done for all sixteen compounds (Figure 6 B).

350 The lack of membrane retention was correctly predicted for THMX and PYME, whereas the

351 lipid phase for the other neutral compounds was overestimated by factors of up to 1.8 (CBZ).

352 The membrane retention was correctly predicted for acids apart from a slight

353 overestimation for compd 2. The discrepancy between predicted and measured membrane

354 retention was generally low except for the lipophilic IM. The full membrane retention for

355 compd 7 and compd 8 was correctly predicted.

356 Predictions for the mass fraction in donor and acceptor were within a range of about 10%

357 deviation (if overestimated lipid fraction is corrected). The only outlier was compd 3 where

358 the measured mass balance did not fit with the prediction (probably due to postulated ion-

359 pairing).

360

361 **Predicting compound distribution within a four compartment model of plant tissues**. After

362 this validation of the cell model (Figure 6) and as a core element of the 'four compartment

363 model' the calculation of mass fractions can be extrapolated to an *in planta* environment.

364 Table 3 summarizes the calculated mass fractions 'at lipids' of the vacuole and cytosol, and

365 the solved fractions of the aqueous phase of all four standardized tissue compartments.

366 These five fractions outline 100% of the mass balance.

367 This type of prediction impressively highlights PYME and THMX as excellent systemic

368 insecticides [15, 18], with low membrane retention and highest distribution in the xylem

369 compared to the other compounds. Acidic compounds are predicted to preferentially

370 distribute in the cytosol and basic phloem compartment (up to 40%). This 'phloem trapping'

371 is well described for phytohormones [23, 35] and herbicides [6]. Basic compounds with log K_{ow}<3

372 were predicted to accumulate in the large, acidic vacuole. This 'vacuole trapping' was

373 recently postulated for both basic insecticides, OX and IM [8, 34]. The vacuolar fraction was

374   drastically reduced with compounds having a log K_{ow}>3 by losing a considerable amount in

375   the membrane retention.

376   This dataset illustrates the mutual influence of log K_{ow} and pK_a on mass distributions. First,

377   the amount distributing in the aqueous phase was highly dependent on the log D. Generally,

378   increasing log K_{ow} increases membrane retention. However, a separate relationship was

379   observed for each compound species: compounds with a log K_{ow} of about 2.3 resulted in a

380   membrane retention of 92% (CBZ) as neutral, of 18% (SPAT enol) as acidic and of 1% (OX) as

381   basic species (Figure 7 A). Second, the distribution within the aqueous phases revealed a pK_a

382   dependent pattern. The predicted quantities solved in vacuoles in relation to the overall

383   solved fractions amounted to 84-85% for neutral compounds, 8-11% for acidic compounds

384   and 98-100% for basic compounds (Figure 7 B). This similarity in behavior of acids on the one

385   hand and of bases on the other hand is due to the quite similar pKa-values in each group

386   (Table 1).

387   Consequently, the absolute amount of a compound solved in one of the four compartments,

388   was dictated by the membrane retention. The relative distribution across the four aqueous

389   phases remains equal within each species of compounds (neutral, acidic, basic).

390

391   **Discussion**

392   In general, PAMPA is used to investigate kinetics of membrane permeation but not to

393   measure equilibrium. This is even more evident when sink conditions are applied to mimic

394   protein binding or blood flow [4]. However, in our context we wanted to simulate a

395   standardized plant cell within the leaf mesophyll and we therefore assumed comparable

396   protein levels in both compartments (i.e. neglecting protein binding). Our results obtained

397   with the PAMPA method cannot be directly transferred to the plant cell scenario since both

398   compartments, donor and acceptor, were of equal volume. In a plant cell the vacuole with

399   about 90% takes the majority of the size. Additionally, the membrane thickness in the

400   PAMPA system is given by the filter dimension carrying the phospholipids. This artificial

401   membrane has a thickness of 125 µm [2] and is therefore about 20'000 times thicker than a 5

402   to 10 nm thick biological lipid bilayer [40]. Accordingly, we would have expected the time

403   needed to reach equilibration within the PAMPA system would be much longer than for a

404   real biological system *in situ*. The relevance of thickness and lipid composition of biological

405   membranes on solute permeability was reviewed by Shinoda (2016) [38].

406

407   The ion trap of weak electrolytes in plants is well documented, but mostly on the macroscale

408   or organismal level. The first tests with pesticides were done by Briggs, Rigitano et al. (1987)

409   [5], where the authors demonstrated that with a series of (weakly acidic) phenoxy acetic acids,

410   both the uptake into barley roots and the translocation to shoots depended on the pH of the

411   external solution and increased with decreasing pH [5, 37]. Later, in a study with (weakly

412   alkaline) phenethylamines and anilines a similar effect but in the opposite direction was

413   demonstrated [25]. This is due to pH differences between external solution and plant cells. If a

414   chemical dissociates in the physiologically relevant range, this influences both uptake

415   velocity and volume. Rendal, Kusk et al. (2011) [36] reviewed 117 ecotoxicology results where

416   toxicity and bioaccumulation of weak acids or bases were tested at multiple pH levels.

417   Toxicity and bioconcentration factors (BCFs) increased for acids at lower pH, the opposite

418   was found for bases. The values of EC50 or BCF changed with pH when pH minus pK_a was in

419   the range of - 1 to 3 for acids, and - 3 to 1 for bases. According to the Henderson-Hasselbalch

420   equation, weak acids and bases occur in both neutral and ionic species in this range, and the

421 effect therefore can be attributed to a change of the ion trap effect. Interestingly single-

422 celled algae also show an effect of pH on toxicity of electrolytes [33].

423

424 Direct *in situ* measurements of the concentration in acidic vacuoles are difficult due to the

425 small size of these intracellular organelles. The authors originally attempted an experimental

426 validation on compound localization in vacuole suspensions isolated from barley [31].

427 However, the required separation steps starting from a protoplast suspension ended many

428 times with concentrations in vacuole fractions too close to the detection limits of test

429 compounds (unpublished results). A recent medical study succeeded in measuring

430 concentrations in lysosomes by using Raman scatter and found an accumulation of the weak

431 bivalent base chloroquine more than 1'000 fold [17]. Our results corroborate these findings.

432 Moreover, we obtained effective permeabilities, and the permeability ratios at varying pH

433 levels which are relevant for the distribution of compounds in the cytosol – vacuole system.

434 Our results are not on the intracellular scale, but mimic those conditions. They can thus be

435 considered as valid for the intracellular distribution in a plant cell. For this, practically no

436 measured concentration values are available. The experimental results of our adapted

437 PAMPA system and the model predictions are generally in very good alignment.

438 Discrepancies were seen for: very lipophilic compounds (that can be explained with the

439 experimental difficulties in detection of such compounds), compd 3 (postulated ion pairing)

440 and compd 5. We can thus use this PAMPA system to obtain data that can be transferred to

441 the intracellular level of plant leaves; and by the application of the model, we can scale-up

442 for the transversal transfer across leaves. This information is highly relevant for the design of

443 modern agrochemicals. Moreover, the consideration of intracellular distribution of

444 compounds is a new and additional way to optimize for more selective plant protection

445 products related to the mode of action and target of a given chemistry. The subcellular

446 distribution of small molecules and related cellular pharmacokinetics retain a great

447 importance in drug design [53].

448

449 The passive permeation of small solutes across lipid membranes is a fundamental process in

450 biology. The membrane permeability of compounds is correlated to their lipophilicity (log

451 K_{ow}). The log K_{ow} for drugs and agrochemicals is typically found below 5 [13]. Agrochemicals

452 show systemic behavior (i.e. long-distance translocation within xylem or phloem) with log

453 K_{ow} below 3 [39]. The mass distributions across plant cell compartments could be well

454 predicted for a broad range of agrochemicals using the presented and now validated model.

455 This makes reference measurements in a PAMPA system obsolete if exceptions in

456 membrane permeability (e.g. ion pairing) could be excluded. Provided that active transport

457 processes mediated through transporters or channels and metabolic transformation are

458 subordinated, the 'four compartment model' offers a great tool for chemistry design and

459 data analysis of biology results in optimization of new agrochemical chemistries.

460

461 **Supporting Information description**

462 The supplement provides the measured data of the equilibrium approach (Table S1), the

463 related calculations on mass fractions (Table S2) and all parameter data for the two

464 compartment model and the expanded four compartment model (Table S3).

References

466   1.   Acosta, E., 3 - Testing the effectiveness of nutrient delivery systems. In *Delivery and*
467   *Controlled Release of Bioactives in Foods and Nutraceuticals*, Garti, N., Ed. Woodhead Publishing:
468   Cambridge, England, 2008; pp 53-106.
469   2.   Assmus, F.; Ross, A.; Fischer, H.; Seelig, J.; Seelig, A., 31P and 1H NMR Studies of the
470   Molecular Organization of Lipids in the Parallel Artificial Membrane Permeability Assay. *Mol. Pharm.*
471   **2017,** *14* (1), 284-295.
472   3.   Avdeef, A.; Bendels, S.; Di, L.; Faller, B.; Kansy, M.; Sugano, K.; Yamauchi, Y., PAMPA--critical
473   factors for better predictions of absorption. *J. Pharm. Sci.* **2007,** *96* (11), 2893-2909.
474   4.   Bermejo, M.; Avdeef, A.; Ruiz, A.; Nalda, R.; Ruell, J. A.; Tsinman, O.; Gonzalez, I.; Fernandez,
475   C.; Sanchez, G.; Garrigues, T. M.; Merino, V., PAMPA--a drug absorption in vitro model 7. Comparing
476   rat in situ, Caco-2, and PAMPA permeability of fluoroquinolones. *Eur. J. Pharm. Sci.* **2004,** *21* (4), 429-
477   441.
478   5.   Briggs, G. G.; Rigitano, R. L. O.; Bromilow, R. H., Physico-chemical factors affecting uptake by
479   roots and translocation to shoots of weak acids in barley. *Pesticide Science* **1987,** *19* (2), 101-112.
480   6.   Bromilow, R. H.; Chamberlain, K.; Evans, A. A., Physicochemical Aspects of Phloem
481   Translocation of Herbicides. *Weed Science* **1990,** *38* (3), 305-314.
482   7.   Buchholz, A.; O'Sullivan, A. C.; Trapp, S., What Makes a Good Compound against Sucking
483   Pests? In *Discovery and Synthesis of Crop Protection Products*, American Chemical Society:
484   Washington, DC, 2015; Vol. 1204, pp 93-109.
485   8.   Buchholz, A.; Trapp, S., How active ingredient localisation in plant tissues determines the
486   targeted pest spectrum of different chemistries. *Pest. Manag. Sci.* **2016,** *72* (5), 929-939.
487   9.   Camenisch, G.; Folkers, G.; van de Waterbeemd, H., Review of theoretical passive drug
488   absorption models: historical background, recent developments and limitations. *Pharm. Acta. Helv.*
489   **1996,** *71* (5), 309-327.
490   10.   Cassayre, J.; Hüter, O.; Hughes, D.; O'Sullivan, A.; Craig, W.; Jacob, O.; Clarke, E.; Earley, F.;
491   Schade, A., Synthesis and Insecticidal Activity of New 2-Aryl-3,5-dihydro-2H-1,4-Benzoxazepine
492   Derivatives. In *Discovery and Synthesis of Crop Protection Products*, American Chemical Society:
493   Washington, DC, 2015; Vol. 1204, pp 391-410.
494   11.   Creemer, L. C.; Giampietro, N. C.; Lambert, W.; Yap, M. C.; deBoer, G. J.; Adelfinskaya, Y.;
495   Castetter, S.; Wessels, F. J., Pro-insecticidal approach towards increasing in planta activity. *Pest.*
496   *Manag. Sci.* **2017,** *73* (4), 752-760.
497   12.   De Duve, C.; De Barsy, T.; Poole, B.; Trouet, A.; Tulkens, P.; Van Hoof, F. o., Lysosomotropic
498   agents. *Biochemical Pharmacology* **1974,** *23* (18), 2495-2531.
499   13.   Delaney, J.; Clarke, E.; Hughes, D.; Rice, M., Modern agrochemical research: a missed
500   opportunity for drug discovery? *Drug. Discov. Today* **2006,** *11* (17-18), 839-845.
501   14.   Eisenach, C.; Francisco, R.; Martinoia, E., Plant vacuoles. *Curr. Biol.* **2015,** *25* (4), R136-R137.
502   15.   Elbert, A.; Haas, M.; Springer, B.; Thielert, W.; Nauen, R., Applied aspects of neonicotinoid
503   uses in crop protection. *Pest. Manag. Sci.* **2008,** *64* (11), 1099-1105.
504   16.   Fischer, H.; Kansy, M.; Avdeef, A.; Senner, F., Permeation of permanently positive charged
505   molecules through artificial membranes--influence of physico-chemical properties. *Eur. J. Pharm. Sci.*
506   **2007,** *31* (1), 32-42.
507   17.   Fu, D.; Zhou, J.; Zhu, W. S.; Manley, P. W.; Wang, Y. K.; Hood, T.; Wylie, A.; Xie, X. S., Imaging
508   the intracellular distribution of tyrosine kinase inhibitors in living cells with quantitative
509   hyperspectral stimulated Raman scattering. *Nat. Chem.* **2014,** *6* (7), 614-622.
510   18.   Fuog, D.; Fergusson, S. J.; Flückiger, C., Pymetrozine: A Novel Insecticide Affecting Aphids and
511   Whiteflies. In *Insecticides with Novel Modes of Action: Mechanisms and Application*, Ishaaya, I.;
512   Degheele, D., Eds. Springer Berlin Heidelberg: Berlin, Heidelberg, 1998; pp 40-49.
513   19.   Goldman, D. E., Potential, Impedance, and Rectification in Membranes. *The Journal of*
514   *General Physiology* **1943,** *27* (1), 37-60.

515   20.   Gulde, R.; Anliker, S.; Kohler, H. E.; Fenner, K., Ion Trapping of Amines in Protozoa: A Novel
516   Removal Mechanism for Micropollutants in Activated Sludge. *Environ. Sci. Technol.* **2018,** *52* (1), 52-
517   60.
518   21.   Gutknecht, J.; Walter, A., Transport of auxin (indoleacetic acid) through lipid bilayer
519   membranes. *J. Membr. Biol.* **1980,** *56* (1), 65-72.
520   22.   Hartmann, T.; Ober, D., Biosynthesis and Metabolism of Pyrrolizidine Alkaloids in Plants and
521   Specialized Insect Herbivores. In *Biosynthesis: Aromatic Polyketides, Isoprenoids, Alkaloids*, Leeper, F.
522   J.; Vederas, J. C., Eds. Springer Berlin Heidelberg: Berlin, Heidelberg, 2000; pp 207-243.
523   23.   Hartung, W.; Slovik, S., Physicochemical properties of plant growth regulators and plant
524   tissues determine their distribution and redistribution: stomatal regulation by abscisic acid in leaves.
525   *New Phytologist* **1991,** *119* (3), 361-382.
526   24.   Hauser, M.-T.; Wink, M., Uptake of Alkaloids by Latex Vesicles and Isolated Mesophyll
527   Vacuoles of Chelidonium ntajus (Papaveraceae). In *Zeitschrift für Naturforschung C*, 1990; Vol. 45, pp
528   949-957.
529   25.   Inoue, J.; Chamberlain, K.; Bromilow, R. H., Physicochemical factors affecting the uptake by
530   roots and translocation to shoots of amine bases in barley. *Pesticide Science* **1998,** *54* (1), 8-21.
531   26.   Kansy, M.; Senner, F.; Gubernator, K., Physicochemical high throughput screening: parallel
532   artificial membrane permeation assay in the description of passive absorption processes. *J. Med.*
533   *Chem.* **1998,** *41* (7), 1007-1010.
534   27.   Kleier, D. A., Phloem mobility of xenobiotics: I. Mathematical model unifying the weak Acid
535   and intermediate permeability theories. *Plant. Physiol.* **1988,** *86* (3), 803-810.
536   28.   Krämer, S. D., Quantitative aspects of drug permeation across in vitro and in vivo barriers.
537   *Eur. J. Pharm. Sci.* **2016,** *87*, 30-46.
538   29.   Lumbroso, A.; Villedieu-Percheron, E.; Zurwerra, D.; Screpanti, C.; Lachia, M.; Dakas, P. Y.;
539   Castelli, L.; Paul, V.; Wolf, H. C.; Sayer, D.; Beck, A.; Rendine, S.; Fonne-Pfister, R.; De Mesmaeker, A.,
540   Simplified strigolactams as potent analogues of strigolactones for the seed germination induction of
541   Orobanche cumana Wallr. *Pest. Manag. Sci.* **2016,** *72* (11), 2054-2068.
542   30.   Martinoia, E.; Massonneau, A.; Frangne, N., Transport processes of solutes across the
543   vacuolar membrane of higher plants. *Plant. Cell Physiol.* **2000,** *41* (11), 1175-1186.
544   31.   Martinoia, E.; Schramm, M. J.; Kaiser, G.; Kaiser, W. M.; Heber, U., Transport of anions in
545   isolated barley vacuoles : I. Permeability to anions and evidence for a cl-uptake system. *Plant Physiol.*
546   **1986,** *80* (4), 895-901.
547   32.   Muller, J.; Esso, K.; Dargo, G.; Konczol, A.; Balogh, G. T., Tuning the predictive capacity of the
548   PAMPA-BBB model. *Eur. J. Pharm. Sci.* **2015,** *79*, 53-60.
549   33.   Neuwoehner, J.; Escher, B. I., The pH-dependent toxicity of basic pharmaceuticals in the
550   green algae Scenedesmus vacuolatus can be explained with a toxicokinetic ion-trapping model.
551   *Aquat. Toxicol.* **2011,** *101* (1), 266-275.
552   34.   O'Sullivan, A. C.; Schaetzer, J. H.; Luethy, C.; Mathews, C. J.; Elliott, C.; Pitterna, T.; Pabba, J.;
553   Jacob, O.; Buchholz, A.; Blythe, J., Synthesis and Insecticidal Activity of New Benzyl- and Indanyl-
554   Oxazolines, Thiazolines and Alkoxy-Alkyl-Imidazolines. In *Discovery and Synthesis of Crop Protection*
555   *Products*, American Chemical Society: Washington, DC, 2015; Vol. 1204, pp 411-430.
556   35.   Raven, J. A., Transport of Indoleacetic Acid in Plant Cells in Relation to pH and Electrical
557   Potential Gradients, and its Significance for Polar IAA Transport. *New Phytologist* **1975,** *74* (2), 163-
558   172.
559   36.   Rendal, C.; Kusk, K. O.; Trapp, S., The effect of pH on the uptake and toxicity of the bivalent
560   weak base chloroquine tested on Salix viminalis and Daphnia magna. *Environ. Toxicol. Chem.* **2011,**
561   *30* (2), 354-359.
562   37.   Rigitano, R. L. O.; Bromilow, R. H.; Briggs, G. G.; Chamberlain, K., Phloem translocation of
563   weak acids in ricinus communis. *Pesticide Science* **1987,** *19* (2), 113-133.
564   38.   Shinoda, W., Permeability across lipid membranes. *Biochimica et Biophysica Acta (BBA) -*
565   *Biomembranes* **2016,** *1858* (10), 2254-2265.

566 39.   Sicbaldi, F.; Attilio Sacchi, G.; Trevisan, M.; A. M. Del Re, A., *Root Uptake and Xylem*
567 *Translocation of Pesticides from Different Chemical Classes*. 1997; Vol. 50, p 111-119.
568 40.   Sitte, P., Die Zelle in der Evolution des Lebens. In *Studium generale: Auf dem Weg zu einem*
569 *allgemeinen Teil der Wissenschaften*, Saner, L., Ed. Springer Fachmedien Wiesbaden: Wiesbaden,
570 2014; pp 137-146.
571 41.   Smolen, V. F., Misconceptions and thermodynamic untenability of deviations from pH-
572 partition hypothesis. *J. Pharm. Sci.* **1973,** *62* (1), 77-79.
573 42.   Sugano, K.; Nabuchi, Y.; Machida, M.; Asoh, Y., Permeation characteristics of a hydrophilic
574 basic compound across a bio-mimetic artificial membrane. *Int. J. Pharm.* **2004,** *275* (1-2), 271-278.
575 43.   Takagi, M.; Taki, Y.; Sakane, T.; Nadai, T.; Sezaki, H.; Oku, N.; Yamashita, S., A new
576 interpretation of salicylic acid transport across the lipid bilayer: implications of pH-dependent but not
577 carrier-mediated absorption from the gastrointestinal tract. *J. Pharmacol. Exp. Ther.* **1998,** *285* (3),
578 1175-1180.
579 44.   Teksin, Z. S.; Hom, K.; Balakrishnan, A.; Polli, J. E., Ion pair-mediated transport of metoprolol
580 across a three lipid-component PAMPA system. *J Control Release* **2006,** *116* (1), 50-57.
581 45.   Teorell, T., Transport processes in membranes in relation to the nerve mechanism. *Exp Cell*
582 *Res* **1958,** *14* (Suppl 5), 83-100.
583 46.   Tischbirek, C. H.; Wenzel, E. M.; Zheng, F.; Huth, T.; Amato, D.; Trapp, S.; Denker, A.; Welzel,
584 O.; Lueke, K.; Svetlitchny, A.; Rauh, M.; Deusser, J.; Schwab, A.; Rizzoli, S. O.; Henkel, A. W.; Muller, C.
585 P.; Alzheimer, C.; Kornhuber, J.; Groemer, T. W., Use-dependent inhibition of synaptic transmission
586 by the secretion of intravesicularly accumulated antipsychotic drugs. *Neuron* **2012,** *74* (5), 830-844.
587 47.   Trapp, S., Bioaccumulation of Polar and Ionizable Compounds in Plants. In *Ecotoxicology*
588 *Modeling*, Devillers, J., Ed. Springer: Boston, MA, 2009; pp 299-353.
589 48.   Trapp, S., Plant uptake and transport models for neutral and ionic chemicals. *Environ. Sci.*
590 *Pollut. Res. Int.* **2004,** *11* (1), 33-39.
591 49.   Trapp, S.; Franco, A.; Mackay, D., Activity-based concept for transport and partitioning of
592 ionizing organics. *Environ. Sci. Technol.* **2010,** *44* (16), 6123-6129.
593 50.   Trapp, S.; Horobin, R. W., A predictive model for the selective accumulation of chemicals in
594 tumor cells. *Eur. Biophys. J.* **2005,** *34* (7), 959-966.
595 51.   Trapp, S.; Rosania, G. R.; Horobin, R. W.; Kornhuber, J., Quantitative modeling of selective
596 lysosomal targeting for drug design. *Eur. Biophys. J.* **2008,** *37* (8), 1317-1328.
597 52.   Yang, Y.-Y.; Toor, G. S.; Williams, C. F., Pharmaceuticals and organochlorine pesticides in
598 sediments of an urban river in Florida, USA. *J. of Soils and Sediments* **2015,** *15* (4), 993-1004.
599 53.   Zheng, N.; Tsai, H. N.; Zhang, X.; Rosania, G. R., The Subcellular Distribution of Small
600 Molecules: From Pharmacokinetics to Synthetic Biology. *Molecular Pharmaceutics* **2011,** *8* (5), 1619-
601 1628.
602
603

604 **Table 1.** Physiochemical properties with compound abbreviation, molecular weight (MW),

605 pK$_a$, log K$_{ow}$ neutral and calculated log D at pH 5.5 and pH 7.0, input parameter for the model

606 with calculated log K$_{ow}$ ion and valency.

	compound	abbr.	chemical properties						model input	
			MW	pK$_a$[a] (base)	pK$_a$[a] (acid)	log K$_{ow}$ neutral	log D (pH 5.5)	log D (pH 7.0)	log K$_{ow}$ ion[b]	Valency[c]
			(g/mol)							
neutral	Pymetrozine	PYME	217	4.1		-0.2	-0.2	-0.2	-3.7	1
	Thiamethoxam	THMX	292	-		-0.1	no pK$_a$	no pK$_a$	-3.6	1
	Cyantraniliprole	CYNT	474		9.1	1.9	1.9	1.9	-1.6	-1
	Carbamazepine	CBZ	236		13.9	2.3	2.3	2.3	-1.3	-1
	Spirotetramat	SPAT	373		10.7	2.5	2.5	2.5	-1.0	-1
acidic	Spirotetramat enol	SPAT enol	301		5.2	2.2	1.7	0.4	-1.3	-1
	Compound 1	compd 1	413		5.1	3.2	2.7	1.3	-0.3	-1
	Compound 2	compd 2	516		5.1	4.4	3.9	2.5	0.9	-1
basic	Compound 3	compd 3	272	9.4		0.3	-3.1	-2.1	-3.2	1
	Oxazoline	OX	220	8.7		2.3	-0.7	0.6	-1.2	1
	Compound 4	compd 4	211	9.1		2.4	-0.8	0.3	-1.1	1
	Compound 5	compd 5	235	9.6		2.6	-0.8	0.1	-0.9	1
	Compound 6	compd 6	237	9.6		3.3	-0.1	0.8	-0.2	1
	Imidazoline	IM	300	9.4		4.3	0.9	1.9	0.8	1
	Compound 7	compd 7	496	7.9		6.3	3.9	5.3	2.4	1
	Compound 8	compd 8	513	7.9		6.8	4.4	5.8	0.4	1

607 [a] pK$_a$ values of PYME, THMX, CYNT, SPAT, SPAT enol, OX, IM were taken from Buchholz and Trapp (2016) [8]; CBZ was
608 taken from Yang (2015) [52]; research compounds were taken from Syngenta internal data base
609 [b] log K$_{ow}$ neutral = log K$_{ow}$ ion + 3.5 from Trapp (2005) [50]
610 [c] z is the electric charge (synonym valency, for acids −, for bases +) [50]

Table 2. Kinetic and equilibrium measurements with the pH gradient conditions pH 7.0 to pH 5.5 and pH 5.5 to pH 7.0. P_e = effective permeability, M_d = Mass fraction in donor, M_a = Mass fraction in acceptor, ND = not determined, N/A = not analyzed (below limit of detection, LOD). Compounds with a difference between M_a and M_d of $\geq$ 15% were marked with "not equilibrated".

		pH 7.0 to pH 5.5			pH 5.5 to pH 7.0			
		kinetic	equilibrium		kinetic	equilibrium		
	compound	P_e	M_a	M_r	P_e	M_d	M_r	comment
		$(10^{-6}$ cm/s)	(%)	(%)	$(10^{-6}$ cm/s)	(%)	(%)	equil. meas.
neutral	Pymetrozine	0.19 ± 0.05	14 ± 2.2	0.0 ± 0.0	0.19 ± 0.01	78 ± 4.9	9.0 ± 4.9	not equilibrated
	Thiamethoxam	0.66 ± 0.13	28 ± 1.8	2.0 ± 1.8	0.65 ± 0.06	72 ± 2.3	1.0 ± 2.1	not equilibrated
	Cyantraniliprole	7.81 ± 1.06	42 ± 2.1	17 ± 5.1	7.41 ± 0.19	40 ± 1.2	22 ± 2.2	
	Carbamazepine	8.82 ± 1.11	N/A	N/A	8.55 ± 0.35	N/A	N/A	
	Spirotetramat	7.45 ± 1.34	26 ± 0.1	48 ± 1.4	11.45 ± 1.05	27 ± 0.6	50 ± 1.2	
acidic	Spirotetramat enol	0.05 ± 0.01	2.0 ± 1.6	4.0 ± 1.5	1.30 ± 0.03	61 ± 5.0	2.0 ± 4.0	not equilibrated
	Compound 1	0.18 ± 0.03	6.0 ± 1.7	0.0 ± 0.0	7.22 ± 0.25	10 ± 0.3	16 ± 0.9	
	Compound 2	0.43 ± 0.05	2.0 ± 2.9	56 ± 4.2	23.20 ± 1.81	2.0 ± 0.1	64 ± 0.7	
basic	Compound 3	0.06 ± 0.01	8.0 ± 8.8	16 ± 7.2	0.05 ± 0.00	98 ± 3.1	1.0 ± 2.4	not equilibrated
	Oxazoline	17.94 ± 4.49	85 ± 0.6	11 ± 10.6	0.58 ± 0.09	89 ± 2.5	4.0 ± 3.2	
	Compound 4	9.58 ± 0.48	81 ± 0.6	12 ± 1.5	0.32 ± 0.02	93 ± 6.9	3.0 ± 4.2	
	Compound 5	8.54 ± 0.94	46 ± 0.6	4.0 ± 4.2	0.45 ± 0.12	100 ± 0.0	0.0 ± 0.0	not equilibrated
	Compound 6	9.55 ± 0.82	78 ± 0.5	17 ± 1.1	0.38 ± 0.02	89 ± 2.0	5.0 ± 4.0	
	Imidazoline	42.46 ± 4.38	52 ± 0.2	45 ± 0.6	0.42 ± 0.07	62 ± 9.8	35 ± 10.2	
	Compound 7	N/A	2.0 ± 0.0	98 ± 2.9	N/A	3.0 ± 0.4	97 ± 0.4	
	Compound 8	N/A	ND	ND	N/A	0.0 ± 0.0	100 ± 0.0	

Table 3. Calculated membrane retention ('at lipid' fractions of cytosol and vacuole) and mass

fractions of aqueous phases in four compartments (solved fraction of phloem, xylem, cytosol

and vacuole). The amount of compound solved in vacuoles in relation to the overall dissolved

fractions is denoted in brackets. Log K_{OW} of neutral species is given.

	compound	log K_{ow}	'at lipids' (vac + cyt) %M_r	solved fractions (aqueous phases of given compartment)			
				%M_{phloem}	%M_{xylem}	%$M_{cytosol}$	%$M_{vacuole}$
neutral	Pymetrozine	-0.2	3.3	2.2	2.8	9.6	82.1 (85%)
	Thiamethoxam	-0.1	4.3	2.3	2.8	10.1	80.5 (84%)
	Cyantraniliprole	1.9	84.0	0.4	0.5	1.7	13.4 (84%)
	Carbamazepine	2.3	91.5	0.2	0.2	0.9	7.1 (85%)
	Spirotetramat	2.5	95.2	0.1	0.1	0.5	4.1 (85%)
acidic	Spirotetramat enol	2.2	18.2	43.0	0.2	31.8	6.9 (8%)
	Compound 1	3.2	67.4	16.7	0.1	13.1	2.7 (8%)
	Compound 2	4.4	97.3	1.2	0.0	1.3	0.3 (11%)
basic	Compound 3	0.3	0.0	0.0	0.9	1.1	98 (98%)
	Oxazoline	2.3	1.1	0.0	1.1	0.4	97.3 (98%)
	Compound 4	2.4	0.9	0.0	0.9	0.7	97.6 (98%)
	Compound 5	2.6	1.0	0.1	0.7	1.6	96.7 (98%)
	Compound 6	3.3	5.3	0.1	0.3	1.5	92.8 (98%)
	Imidazoline	4.3	35.1	0.0	0.0	0.7	64.1 (99%)
	Compound 7	6.3	99.7	0.0	0.0	0.0	0.3 (100%)
	Compound 8	6.8	99.9	0.0	0.0	0.0	0.1 (100%)

621

622 **Figure 1.** Structures of tested agrochemicals, drugs and research compounds.

623

624 **Figure 2.** Schematic illustration of the compound diffusion from the donor to the acceptor

625 compartment (Volume 50:50) in a pH gradient with buffer A and buffer B.

626

627 **Figure 3.** Effective permeabilities (P_e) measured from pH 7.0 to pH 5.5 and pH 5.5 to pH 7.0

628 in the kinetic PAMPA approach (18 h). The error bars represent the standard sample

629 deviation.

630

631 **Figure 4.** Correlation between the difference of log D between donor and acceptor

632 compartment (Δ log D) and the difference of log P_e from pH 5.5 to pH 7.0 and *vice versa*

633 (Δ log P_e) measured in the kinetic approach.

634

635 **Figure 5**. Figure 5. Mass fractions of the aqueous phase in the acidic compartment (pH 5.5)

636 after thermodynamic equilibration. This means the mass fractions are given without the

637 membrane retention (see Equation 3) in donor ($M_{d,aq}$) and acceptor ($M_{a,aq}$) in pH gradient

638 direction from pH 5.5 to pH 7.0 and pH 7.0 to pH 5.5, respectively. The dotted lines represent

639 the average mass fraction of compound species in the acidic compartment: neutral 51%,

640 acidic 15% and basic 86%. Not equilibrated compounds are marked with an asterisk. The

641 error bars represent the standard sample deviation.

642

643 **Figure 6.** Mass fractions at equilibrium for donor (M_d), acceptor (M_a) and membrane

644 retention (M_r). (A) Mass fractions calculated with the 'PAMPA cell model'. (B) Mass

645 distributions measured with PAMPA (see Method).

646

647 **Figure 7.** Impact of log K_{ow} and pK_a on mass distributions in 'at lipids' and in solved

648 fractions (Table 3). (A) Correlation between log K_{ow} and membrane retention related to

649 compound species. The dotted lines represent the membrane retention tendency for each

650 compound species. (B) Correlation between log K_{ow} and mass fraction in vacuoles relative to

651 total aqueous phase for each compound species. The dotted lines represent the average for

652 each compound species.

653
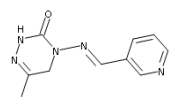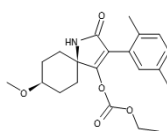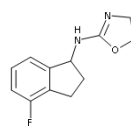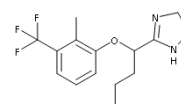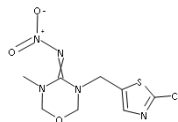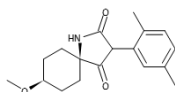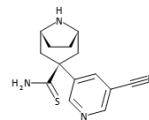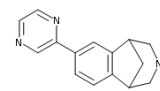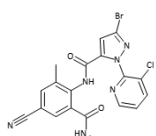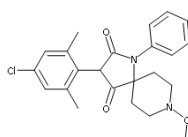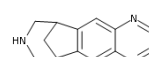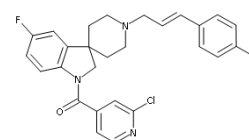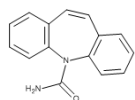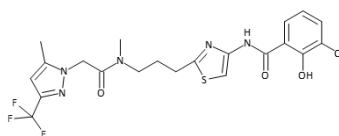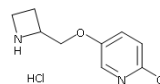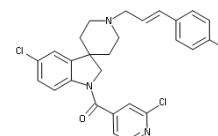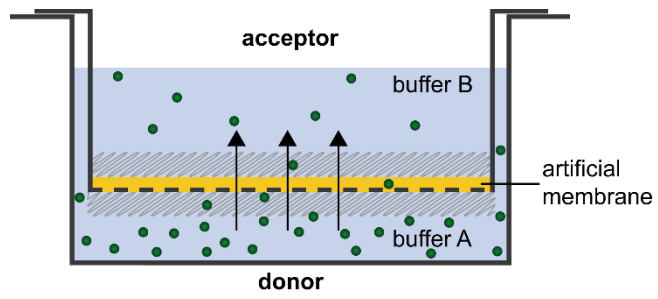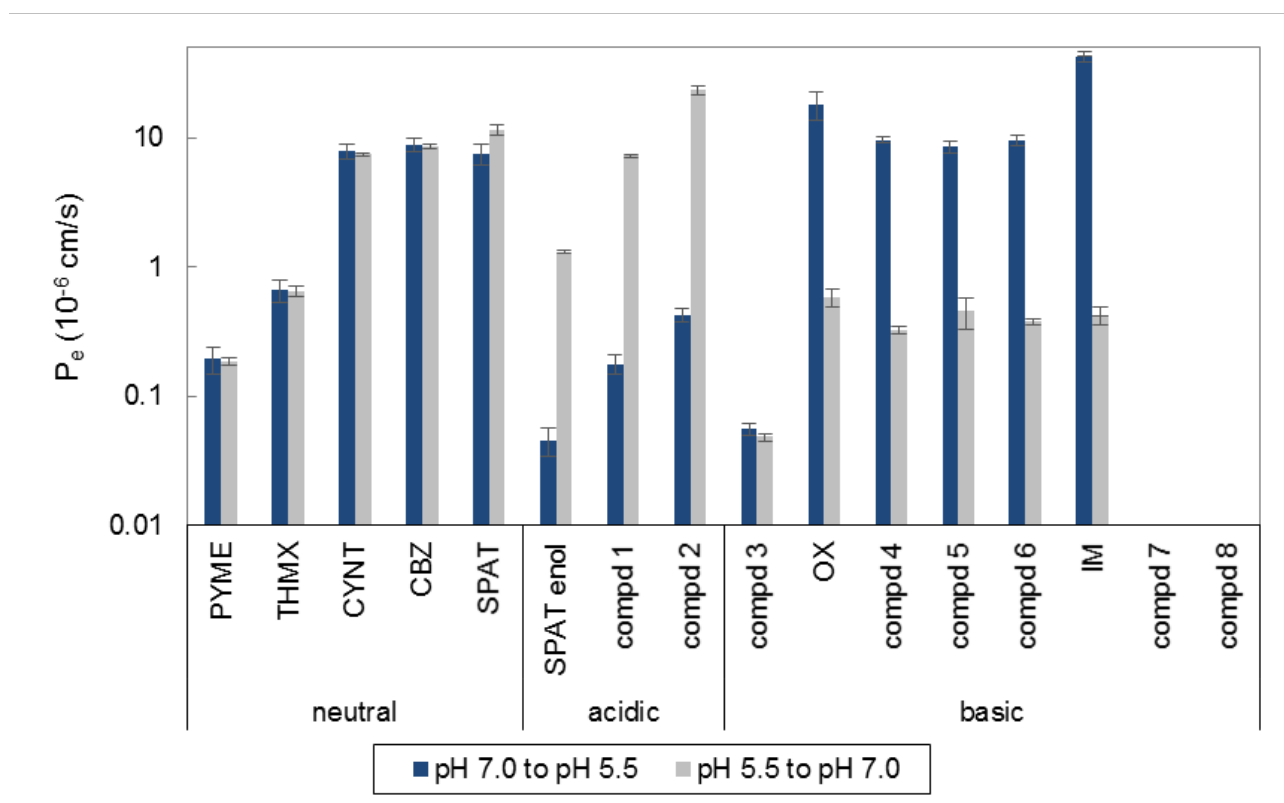
Figure 1.

Figure 2.

Figure 3.

Figure 4.

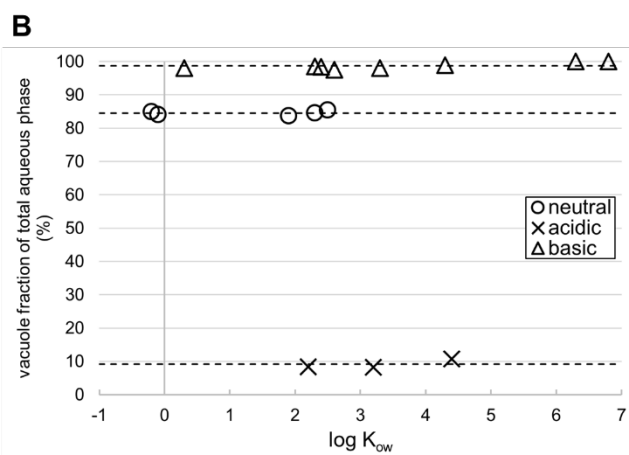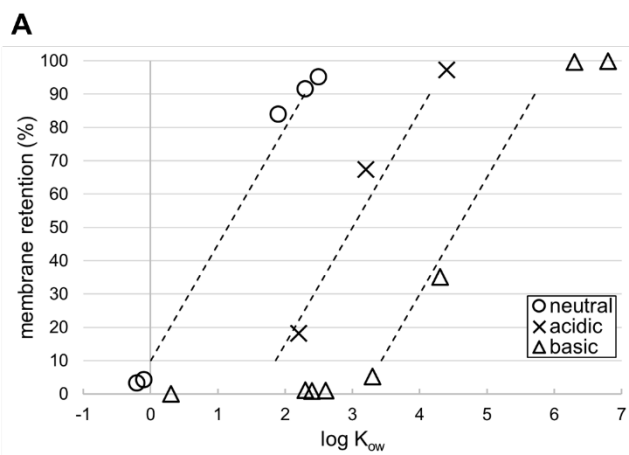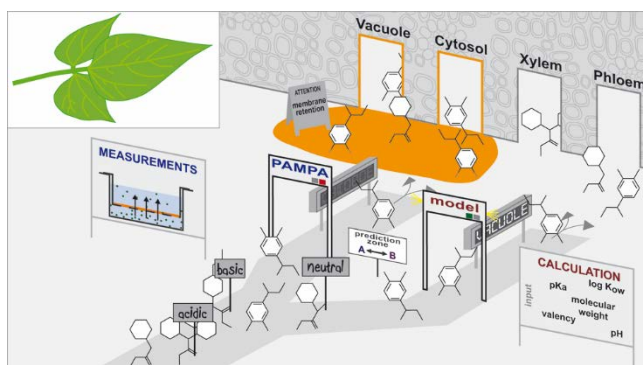**Figure 5**.

Figure 6.

654

Figure 7.

656
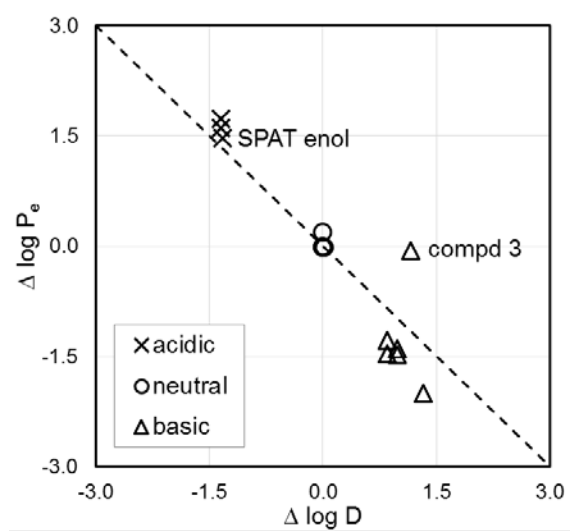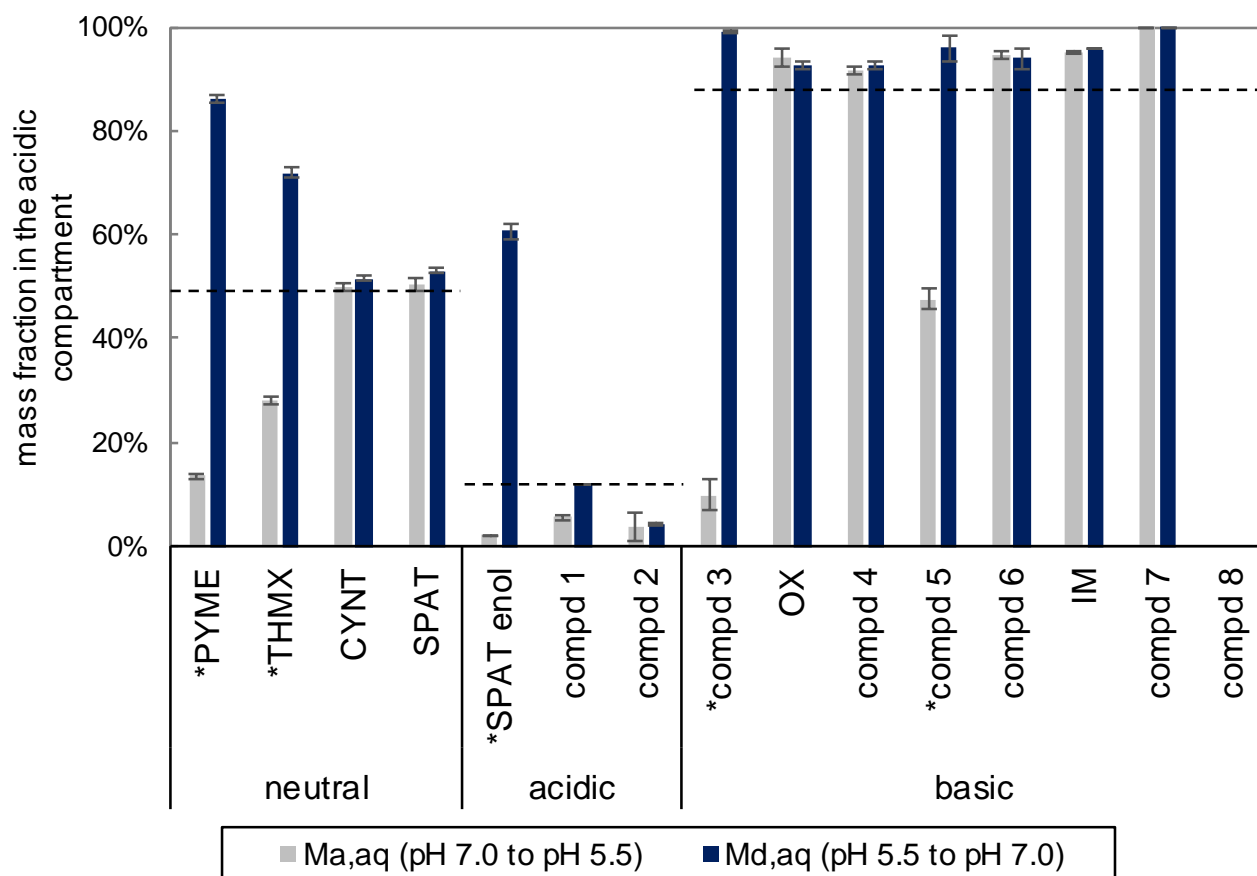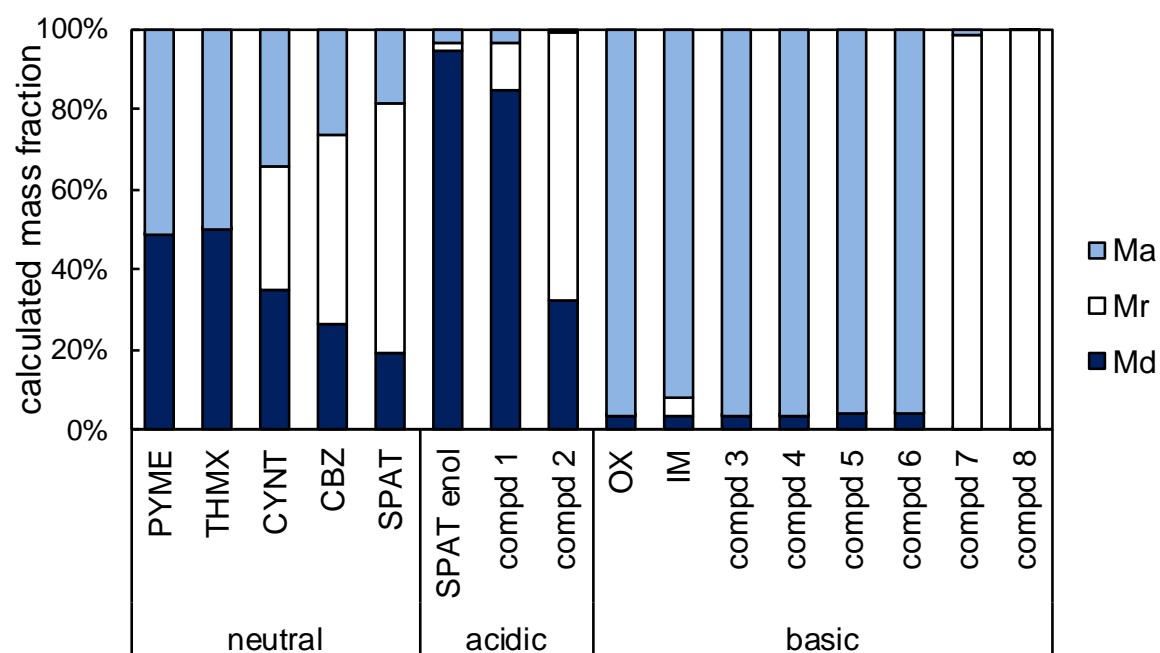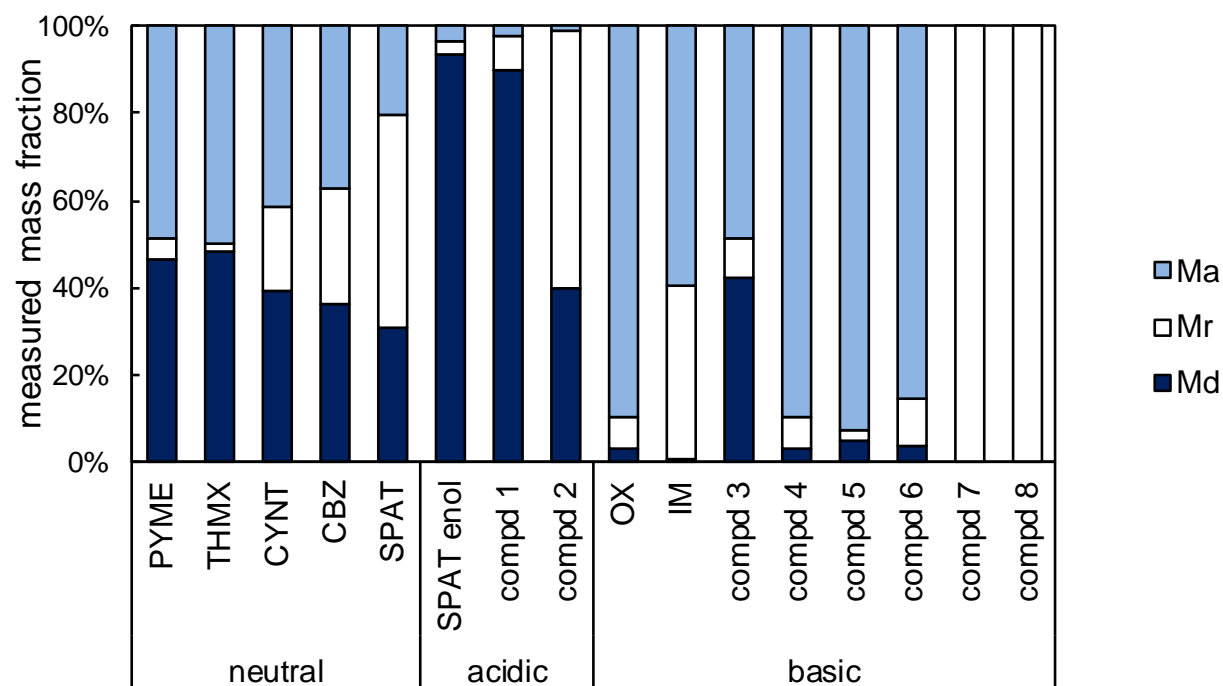
657   **Table of Contents graphic**

658

659

660

661